Effects of antimicrobial Ti6Al4V-Ag implants and hMSCs on osteoclastogenesis

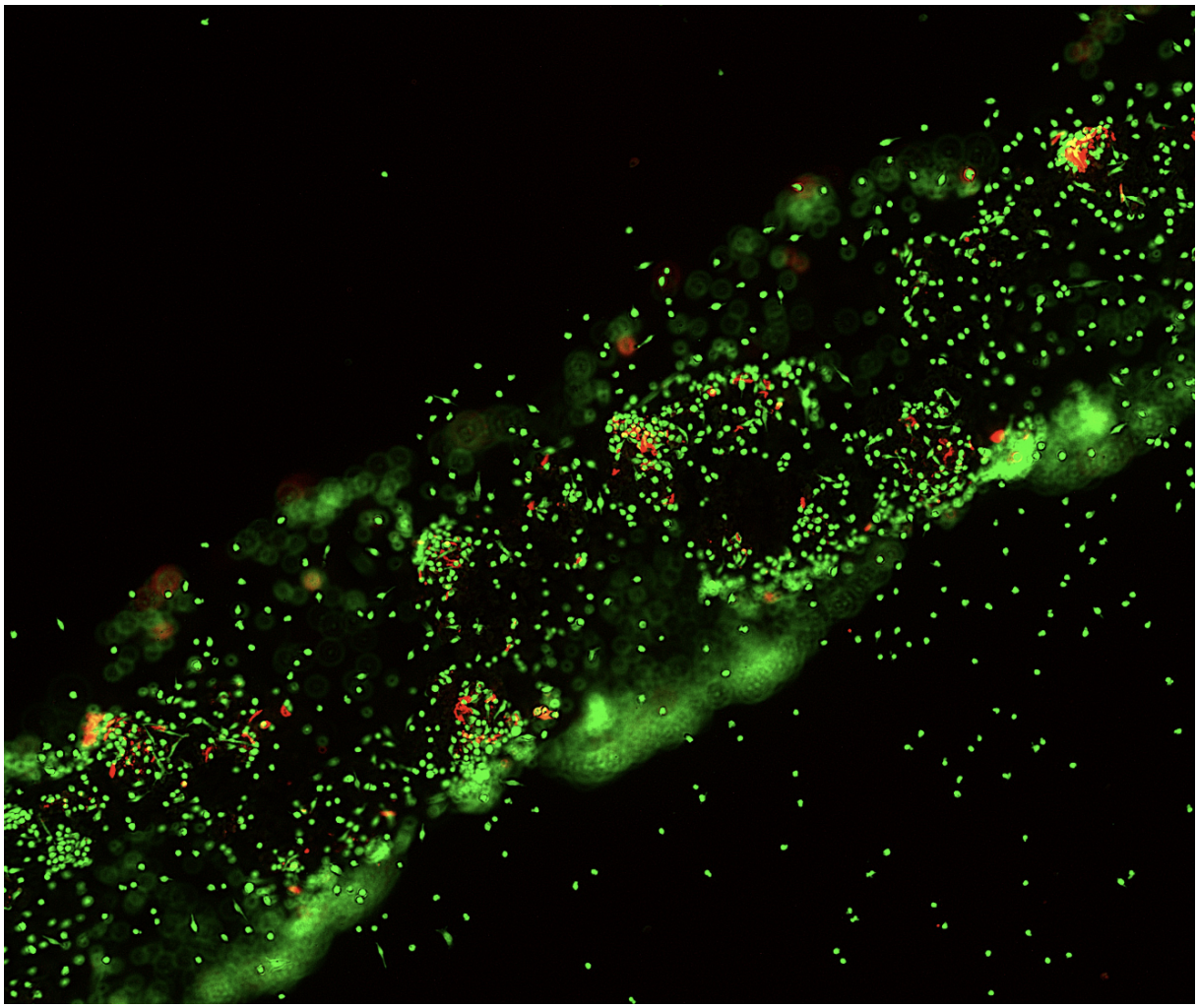

Master Thesis

Kacper Mirkowski Andersen

03/2025-03/2026

Effects of antimicrobial Ti6Al4V-Ag implants and hMSCs on osteoclastogenesis

by

Kacper Mirkowski Andersen
6051111

in partial fulfilment of the requirements for the degree of

Master of Science
in Mechanical Engineering

at the Delft University of Technology,
to be defended publicly on Friday March 6, 2026 at 10:30 AM.

Supervisors:	Dr. Ir. I. Apachitei (TU Delft)
	Dr. ir. E.L. Fratila-Apachitei (TU Delft)
	Prof. E. Farrell (Erasmus MC)
	Msc. A. Garmendia Urdalleta (Erasmus MC)
Thesis Committee:	Dr.ir. R. de Kruijff (TU Delft)

Biomechanical Engineering Department
Faculty of Mechanical Engineering
Delft University of Technology

Abstract

Implant-associated infections remain a major challenge in orthopaedic surgery, motivating the development of antimicrobial implant surfaces that do not compromise bone regeneration. As osteoclasts are crucial for bone remodelling and implant integration, their response to antimicrobial surface modifications must be carefully evaluated. This thesis investigated the effects of silver nanoparticles (AgNPs) incorporated into plasma electrolytic oxidation (PEO) treated Ti6Al4V implant surfaces on osteoclastogenesis under direct and indirect in vitro exposure conditions. Human CD14+ monocytes were cultured directly on the implant surfaces to evaluate surface-mediated effects, and indirectly in Transwell-based mono- and coculture models to assess the influence of released ions and human mesenchymal stem cell (hMSC)-derived signals on osteoclastogenesis. Surface characterisation confirmed successful PEO treatment and AgNP incorporation without alteration of surface morphology. Direct contact with AgNP-containing surfaces reduced the number of viable adherent cells, while osteoclast differentiation markers remained detectable in surviving cells. In contrast, indirect exposure to implant-derived ionic cues did not impair osteoclast formation. These findings highlight the exposure-dependent effects of AgNP-incorporated PEO surfaces and support their potential for antimicrobial implant design within a biologically tolerable range.

Contents

1 Introduction **1**

2 Materials & Methods **4**

2.1 Implants . . . 4

2.1.1 Design and fabrication . . . 4

2.1.2 Surface biofunctionalisation . . . 5

2.1.3 Surface characterisation . . . 6

2.2 Cell isolation and seeding . . . 6

2.2.1 Implant preparation for culturing . . . 6

2.2.2 Monocyte isolation . . . 6

2.2.3 Monocyte seeding and culturing on implants and in monolayer . . . 7

2.2.4 hMSC isolation and expansion . . . 7

2.3 Indirect coculture of hMSCs and monocytes . . . 8

2.4 Monocyte and osteoclast viability . . . 9

2.5 DNA quantification . . . 10

2.6 Osteoclast visualisation and quantification . . . 10

2.7 Gene expression analysis of osteoclasts . . . 11

2.8 Calcium concentration in culture medium . . . 13

2.9 Statistical analysis . . . 13

3 Results **14**

3.1 Surface biofunctionalisation of Ti6Al4V implants . . . 14

3.2 Effects of M-CSF in culture medium on monocyte viability . . . 15

3.3 Effects of AgNPs incorporated in PEO treated implants on osteoclast viability . . . 16

3.4 Effects of silver ion release from PEO-treated implants on osteoclastogenesis . . . 17

3.5 Effects of AgNPs incorporated in PEO treated implants on osteoclast viability when cocultured indirectly with hMSCs . . . 19

4 Discussion **21**

4.1 Surface biofunctionalisation of Ti6Al4V implants . . . 21

4.2 Effects of M-CSF in culture medium on monocyte viability . . . 22

4.3 Effects of AgNPs incorporated in PEO-treated implants on osteoclast viability . . . 22

4.4 Effects of silver ion release from PEO-treated implants on osteoclastogenesis . . . 23

4.5 Effects of AgNP PEO-treated implants under indirect coculture conditions . . . 24

4.6 Implications for implant surface design . . . 25

4.7 Limitations . . . 26

4.8 Recommendations for future work . . . 26

5 Conclusion **27**

References **28**

A Appendix **31**

A.1 Investigation of a consensus media for a coculture with hMSCs and osteoclasts . 31

Introduction 1

Orthopaedic implants play a crucial role in restoring mobility and quality of life for a wide range of patients. As life expectancy increases, the number of arthroplasty procedures continues to rise. In the Netherlands, total hip replacements increased from 8,902 in 2007 to 36,684 in 2023 [1]. Although advances in surgical techniques and biomaterials have significantly improved implant longevity since the first total joint arthroplasty [2], early implant failure remains a persistent clinical challenge. Among the complications that arise within the first two years after surgery, implant-associated infections (IAIs) form the largest category, accounting for approximately 31% of short-term failures following primary hip arthroplasty [3].

A key difficulty in managing IAIs stems from the ability of bacteria to rapidly colonise implant surfaces and form biofilms. Once bacteria adhere to an implant, they secrete an extracellular polymeric substance that creates a physical and biochemical barrier against immune cells and antibiotics [4]. Biofilm-embedded bacteria can tolerate antibiotic concentrations up to 1,000 times higher than planktonic bacteria [5], making pharmacological treatment alone insufficient in many cases. Consequently, surgical revision—often involving implant removal, debridement, and extended antibiotic therapy—remains the standard treatment for persistent infections. The development of implant surfaces that can prevent bacterial colonisation from the outset has therefore become a priority in orthopaedic biomaterials research [6].

To address these challenges, implant surface modification strategies employing alternative antimicrobial agents have attracted significant attention. Silver is one of the most widely investigated materials due to its broad-spectrum antimicrobial activity, longstanding clinical use, and low tendency to induce bacterial resistance [7]. Silver nanoparticles (AgNPs) in particular exhibit enhanced reactivity and high surface-area-to-volume ratios, enabling potent antimicrobial effects at relatively low concentrations [8, 9]. Their mechanisms include disruption of bacterial cell walls, interference with metabolic pathways, and the generation of reactive oxygen species.

A surface modification technique that has become increasingly relevant in this context is Plasma Electrolytic Oxidation (PEO). PEO is an electrochemical process that, when applied to titanium alloys such as Ti6Al4V, forms a thick oxide layer enriched with micro- and nanopores [10]. These pores substantially increase the surface area for protein adsorption, improve wettability, and promote osteogenic cell attachment and migration. Importantly, the porous oxide layer produced by PEO can incorporate bioactive ions or nanoparticles directly into the oxide layer [11]. This makes PEO a particularly attractive platform for combining osteoconductive surface properties with antibacterial functionality. By embedding AgNPs within the PEO-generated structure, implants can provide both surface antimicrobial activity and a release of silver ions over time.

However, while AgNP-functionalised surfaces show strong potential for preventing bacterial adhesion, their effects on host cell behaviour must be carefully evaluated. A fundamental aspect of implant success is osseointegration, the process by which bone establishes a direct and stable interface with the implant surface [12]. Immediately after implantation, the surgical defect fills with blood, and serum proteins rapidly adsorb onto the titanium surface, forming a provisional matrix that guides subsequent tissue regeneration [13]. Platelet activation initiates the release of cytokines and growth factors including PDGF and TGF-β, which draw immune cells and subsequently osteogenic progenitors to the site.

Osteoclasts (OC) play an important role in bone regeneration. They are multinucleated, bone resorbing cells derived from monocytes. During the early inflammatory phase of healing, circulating monocytes are recruited to the injury site, where they primarily differentiate into macrophages as part of the innate immune response. Under the influence of key osteoclastogenic factors, particularly macrophage colony-stimulating factor (M-CSF) and receptor activator of nuclear factor-κB ligand (RANKL), these monocyte/macrophage lineage cells can subsequently fuse and differentiate into mature osteoclasts responsible for bone resorption [14]. Their activity begins early in the proliferative phase of healing, when necrotic bone created during drilling undergoes resorption. Both newly differentiated osteoclasts derived from recruited monocytes and pre-existing osteoclasts on adjacent bone surfaces contribute to this early remodelling process. Activated osteoclasts attach to the cut bone edges and dissolve mineralised matrix through acidification and the release of proteolytic enzymes such as cathepsins and Matrix Metalloproteinases (MMPs). This resorptive activity not only removes damaged bone but also releases matrix-bound signalling molecules including BMPs, PDGF, and TGF-β, which stimulate osteogenic differentiation and angiogenesis [13]. Thus, osteoclasts help create the microenvironment required for new bone deposition.

Beyond bone regeneration, osteoclasts remain essential during the remodelling phase, where woven bone is replaced with mechanically stronger lamellar bone [15]. The coordinated coupling of osteoclast-mediated resorption and osteoblast-mediated formation enables the bone–implant interface to adapt structurally to mechanical loading. Impairments in osteoclast number, viability, or function can disrupt this balance, leading to delayed integration, inadequate bone turnover, or long-term instability of the implant [16].

Despite their central role in osseointegration, osteoclast responses to silver-modified implant surfaces remain insufficiently understood. While AgNPs are effective in preventing bacterial colonisation, they may influence monocyte survival, osteoclast differentiation, or resorptive capacity. Because osteoclasts directly influence early bone turnover and long-term remodelling around the implant, evaluating their behaviour in the presence of AgNP-containing PEO surfaces is critical. Understanding these interactions is essential to ensure that the antimicrobial benefits of silver do not compromise the biological processes required for stable and functional implant integration.

In addition to their surface-mediated effects, previous studies have demonstrated that AgNP-containing PEO treated Ti6Al4V implants release silver ions, as well as calcium- and phosphate-

ions, into the surrounding medium over time [17]. These ions may influence monocyte survival, differentiation, or signalling even when no direct cell–implant contact takes place [18]. Because osteoclastogenesis is strongly regulated by soluble factors present in the local microenvironment, it is essential to assess both direct and indirect effects of AgNP-containing PEO implants on osteoclast formation. Indirect effects can arise not only from silver ion release but also from the presence of osteogenic human mesenchymal stem cells (hMSCs) at the implant interface. Although the effects of AgNP-modified surfaces on hMSC and human macrophage behaviour have been examined in earlier studies [19, 20], the role of hMSCs present at the implant interface on osteoclastogenesis remains unclear. Through the secretion of cytokines and growth factors, hMSCs can modulate osteoclastogenesis indirectly by shaping the local balance of pro- and anti-osteoclastogenic signals, including factors involved in M-CSF– and RANKL-mediated pathways [21].

The aim of this thesis was to investigate the biological effects of AgNPs incorporated into PEO-treated Ti6Al4V implants on osteoclast-related cellular responses using human primary cells.

To address this aim, a combination of direct and indirect *in vitro* culture models is employed. In the direct culture model, monocytes are seeded directly onto the implant surfaces, allowing assessment of cell responses influenced by surface chemistry, topography, and locally released silver ions. In contrast, indirect culture models are used to isolate the effects of soluble factors, in which the monocytes are not in physical contact with the implant surface but are instead exposed only to implant- or cell-derived molecules that diffuse through the culture medium via a Transwell system. This approach enables evaluation of silver ion release and paracrine signalling while excluding direct surface-mediated interactions. To capture the possible effects of hMSCs on osteoclastogenesis, a coculture model was established. The hMSCs were precultured on the implants before they were exposed to monocytes in a Transwell system.

Specifically, this study has a two-fold objective:

1. To determine how silver nanoparticles incorporated into PEO-treated Ti6Al4V implants influence monocyte attachment, viability, and differentiation into osteoclasts.
2. To identify the role of hMSCs cultured on the implants on osteoclastogenesis.

Materials & Methods 2

2.1 Implants

2.1.1 Design and fabrication

The Ti6Al4V implants used in this study were additively manufactured based on a previously established, rationally designed geometry optimised for biological evaluation [22]. The implants consisted of a high-aspect-ratio, wire-like structure (40 mm in length and 0.5 mm in diameter), selected to maximise surface area while maintaining mechanical integrity and suitability for subsequent surface biofunctionalisation (Figure 2.1A).

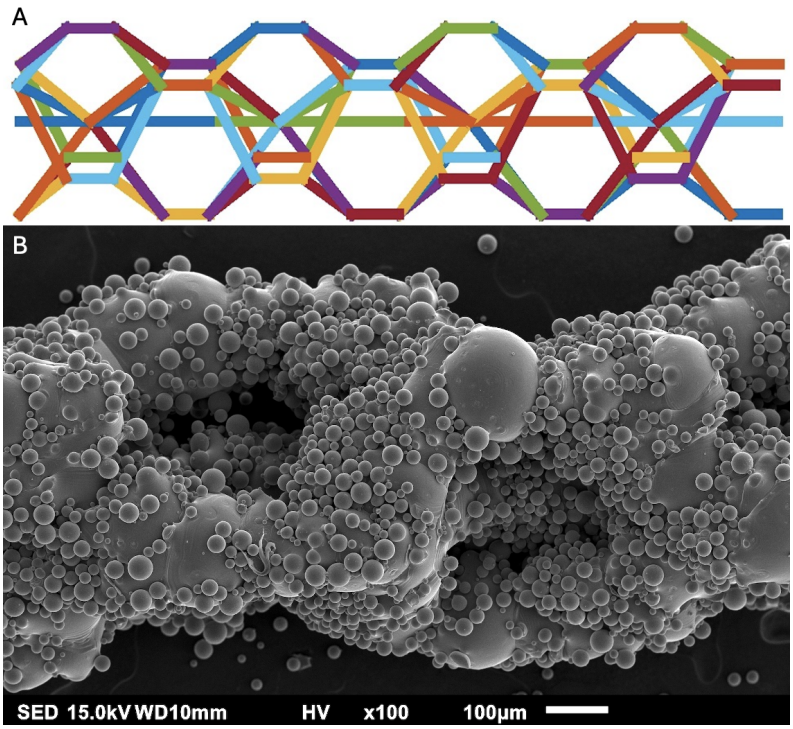

Figure 2.1. (A) Schematic representation of the implant geometry (Adapted from [22]). (B) SEM image of the as-fabricated Ti6Al4V implant surface prior to PEO treatment.

All implants were produced at the Additive Manufacturing Laboratory (TU Delft, The Netherlands) using Selective Laser Melting (SLM). Fabrication was performed on a Realizer SLM-125 system (Borchem, Germany) equipped with a YLM-400-AC ytterbium fibre laser (IPG Photonics, Oxford, United States). Printing took place under an inert argon atmosphere with oxygen levels maintained below 0.2%. Medical-grade (grade 23, ELI) Ti6Al4V spherical particles ranging from 10–45 μm in diameter (AP&C, Boisbriand, Quebec, Canada) served as the feedstock material.

Following fabrication, residual powder was removed, and the implants were cleaned by sequential ultrasonication in acetone, 96% ethanol, and demineralised water to ensure surface cleanliness prior to biofunctionalisation and cell culture experiments (Figure 2.1B).

2.1.2 Surface biofunctionalisation

The implants were biofunctionalised by PEO at the Biofunctionalisation Laboratory (TU Delft, Delft, The Netherlands). Prior to PEO treatment, the implants were mounted in crocodile clip holders and partially masked with waterproof tape to define and standardise the exposed surface area. This approach ensured consistent electrochemical processing across all samples.

PEO was performed in a double-walled electrochemical cell placed on a cooled magnetic stirrer (Figure 2.2). The cathode was thoroughly rinsed with demineralised water prior to each experiment. The electrolyte consisted of demineralised water containing 24 g/L calcium acetate and 4.2 g/L calcium glycerophosphate.

For silver-containing samples, silver nanoparticles (Sigma-Aldrich, St. Louis, USA) were added to the electrolyte at a concentration of 0.3 g/L. To ensure even dispersion of the nanoparticles, the electrolyte was sonicated twice for 5 min prior to use.

Once the electrolyte temperature reached $\leq 6°C$, the implants were immersed such that only the intended surface area was exposed to the electrolyte. The implants served as the anode in the electrochemical system. PEO processing was carried out using a 50 Hz AC power supply (ACS 1500, ET Power Systems Ltd., UK), with voltage–time transients recorded via an SCXI data acquisition module (National Instruments, USA). A current density of 20 A/dm^2 (corresponding to 389 mA per implant) was applied for 5 min. Throughout the process, electrolyte temperature was maintained using a recirculating chiller (Thermo Haake V15, Germany).

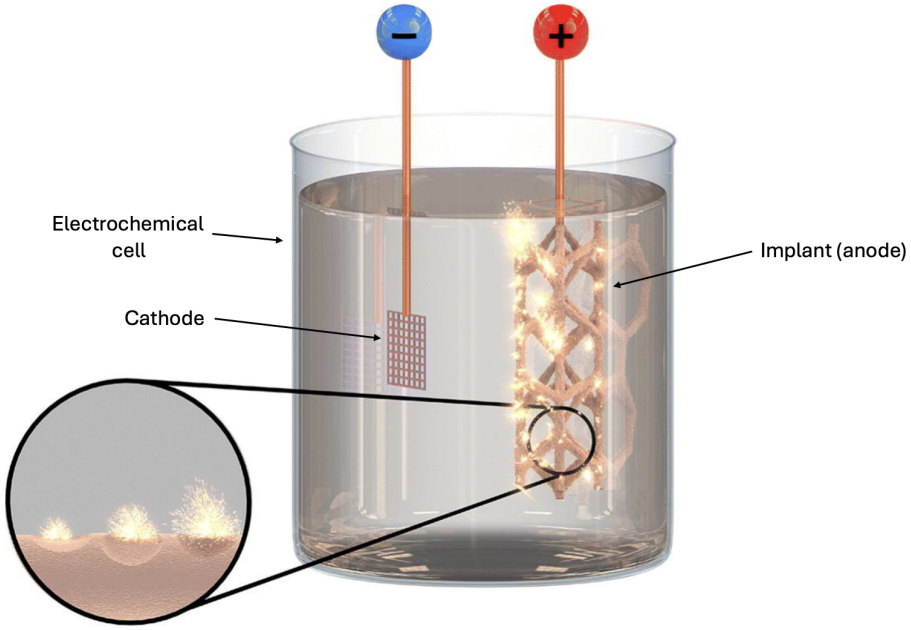

Figure 2.2. Schematic representation of the biofunctionalisation setup. Figure adapted from [23].

Following completion of the PEO process, the implants were rinsed with water to remove residual electrolyte and subsequently prepared for surface characterisation and cell culture experiments.

2.1.3 Surface characterisation

The surface morphology and chemical composition of the implants were evaluated to confirm successful PEO treatment and AgNP incorporation. Surface imaging was performed using a scanning electron microscope (SEM; JSM-IT100LV, JEOL, Tokyo, Japan). Prior to imaging, the implants were sputter-coated with a thin gold layer for 30 s to improve surface conductivity and image quality. SEM imaging was conducted at a electron beam energy of 15 kV and a working distance of 10 mm, allowing detailed visualisation of the micro- and nanoporous oxide layers generated by the PEO process. For each PEO batch, images were taken length wise at a magnification ranging between 100x-800x.

To assess the elemental composition of the surfaces and verify the presence of silver, energy-dispersive X-ray spectroscopy (EDS) was performed. Point analysis mode was used, in which a focused electron beam excites the electronic structure of atoms within a defined small region of the surface, generating characteristic X-ray emissions that enable elemental identification [24]. The resulting spectra were examined to confirm the presence of calcium and phosphorus, as well as silver associated with the PEO and PEO+AgNP samples.

These combined imaging and analytical methods ensured that both the morphological and chemical features of the functionalised surfaces were accurately characterized prior to cell culture experiments.

2.2 Cell isolation and seeding

2.2.1 Implant preparation for culturing

Following the PEO treatment, the implants were cut into 1 cm long segments and transferred into autoclave-safe sterilisation tubes. Sterilisation was performed in an autoclave at 121°C for 15 min to inactivate bacteria, viruses, and other viable microorganisms prior to cell culture. After sterilisation, the implants were placed in a 37°C oven and dried overnight.

To evaluate the influence of the initial burst release of silver ions from PEO+AgNP samples on the studied cells, some implants were pre-soaked prior to cell seeding. Therefore, the samples were immersed in sterile 0.9% NaCl solution for 48 h.

2.2.2 Monocyte isolation

Human $CD14^+$ were isolated from buffy coats left over from voluntary whole blood donations after informed consent of the donors (all males) according to the regulations of Sanquin (Dutch Bloodbank Service). Buffy coats were anonymised prior to delivery from Sanquin to ErasmusMC.

The monocytes were isolated using a combination of density gradient separation and magnetic-activated cell sorting (MACS) [19]. Following isolation, monocytes were cryopreserved in a freezing medium consisting of 20% dimethyl sulfoxide (DMSO; Sigma-Aldrich, St. Louis, USA) in fetal bovine serum (FBS; Sigma-Aldrich, St. Louis, USA). The cell suspensions were gradually cooled and stored in liquid nitrogen at −196°C until required for experimental use.

2.2.3 Monocyte seeding and culturing on implants and in monolayer

Cryopreserved monocytes were thawed rapidly in a 37°C water bath and transferred immediately into a 50 mL Falcon tube containing pre-warmed osteoclast medium. The medium consisted of αMEM (Gibco, ThermoFisher Scientific, Breda, The Netherlands) supplemented with heat inactivated 15% FBS, 50 μg/mL gentamycin (Gibco, ThermoFisher Scientific, Breda, The Netherlands), 0.25 μL/mL amphotericin B (Gibco, ThermoFisher Scientific, Breda, The Netherlands), and 25 ng/mL human macrophage colony-stimulating factor (M-CSF; R&D Systems, Minneapolis, MN, USA). The cells were centrifuged at 300 g for 8 min, resuspended in fresh medium, and cell viability was assessed by Trypan blue exclusion and a Bürker-Türk haemocytometer.

For implant seeding, three implant samples were placed into a 0.2 mL Eppendorf tube. The monocyte suspension was adjusted to a density of 1×10^7 cells/mL medium, and 100 μL of this suspension was carefully pipetted onto the implants. The tubes were incubated for 2 h at 37°C and 5% CO_2, with rotation every 30 min to promote uniform cell attachment (Figure 2.3). After incubation, implants were transferred using sterile forceps into non-adherent 24-well plates (ThermoFisher Scientific, Denmark) containing 500 μL of osteoclast medium per well.

For monolayer cultures, monocytes were thawed and seeded directly into standard 24-well plates at a density of 1.5×10^5 cells/cm^2 in 500 μL osteoclast medium. On day 3, all the samples were refreshed with osteoclast medium supplemented with 30 ng/mL recombinant receptor activator of nuclear factor κB ligand (RANKL; Peprotech Cranbury, NJ, USA) to induce osteoclast differentiation. Cultures were maintained at 37°C and 5% CO_2, with medium changes performed every 3–4 days.

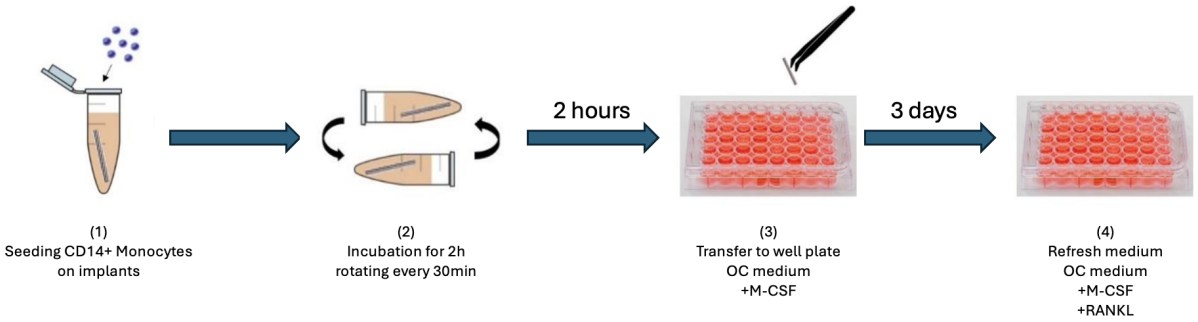

Figure 2.3. Overview of the seeding process of CD14+ monocytes on implants

2.2.4 hMSC isolation and expansion

Human mesenchymal stem cells (hMSCs) were isolated from leftover iliac crest bone chips obtained from paediatric patients undergoing cleft palate reconstructive surgery, following an established isolation protocol [25]. All procedures were approved by the Medical Ethics Committee

of Erasmus MC. Cells were thawed and expanded at passages 2–4 prior to use in experiments.

Thereafter, frozen hMSCs were thawed and seeded into T175 culture flasks (Falcon, St. Louis, USA) at an initial density of 2,300 cells/cm^2. Cells were cultured in complete expansion medium consisting of αMEM supplemented with heat inactivated 10% FBS, 50 μg/mL gentamycin, 1.5 μg/mL amphotericin B, 25 μg/mL L-ascorbic acid 2-phosphate (Sigma-Aldrich, St. Louis, USA), and 1 ng/mL fibroblast growth factor-2 (FGF-2; Instruchemie, Delfzijl, The Netherlands).

Cultures were maintained at 37°C and 5% CO_2, with medium changes every 3–4 days. Cells were expanded until reaching 80–90% confluence, after which they were detached using 3ml per flask of 0.25% trypsin-EDTA solution (Gibco, ThermoFisher Scientific, Breda, The Netherlands) and prepared for experimental seeding.

2.3 Indirect coculture of hMSCs and monocytes

hMSCs were isolated and expanded as described in Section 2.2.4. Following implant cutting and sterilisation, individual implant segments were placed into sterile 0.2 mL tubes using autoclaved forceps (one implant per tube). hMSCs were detached using trypsin (Gibco, ThermoFisher Scientific, Breda, The Netherlands) and resuspended in complete expansion medium. A total of 1.5×10^5 cells in 100 μL medium were seeded directly onto each implant-containing tube. The tubes were incubated for 2 h at 37°C and 5% CO_2, with rotation every 30 min to facilitate uniform cellular attachment (Figure 2.4).

After this initial seeding period, three implants were transferred into each well of a non-adherent 24-well plate containing 500 μL complete expansion medium per well and cultured for an additional 24 h. The following day, implants were moved into a new non-adherent 24-well plate containing 250 μL complete osteogenic medium per well. The osteogenic medium consisted of high-glucose DMEM (Gibco, ThermoFisher Scientific, Breda, The Netherlands), heat inactivated 10% FBS, 50 μg/mL gentamycin, 1.5 μg/mL amphotericin B, and freshly added supplements: 0.1 μM dexamethasone, 0.1 mM L-ascorbic acid 2-phosphate, and 10 mM sodium-β-glycerophosphate (Sigma-Aldrich, St. Louis, USA).

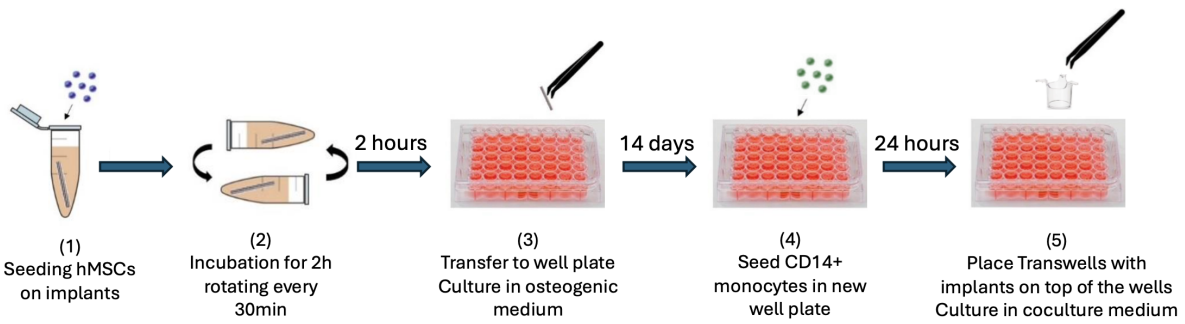

Figure 2.4. Overview of the seeding and culturing process of hMSCs and CD14+ monocytes for the coculture experiments.

In parallel, a monolayer osteogenic control was prepared in a 6-well plate at a density of 3,000 cells/cm^2 in 1.5 mL medium and incubated for 24 h at 37°C, 5% CO_2. The next day, these control wells were refreshed with either complete osteogenic medium (three wells) or non-osteogenic medium (three wells; high-glucose DMEM with 10% FBS, 50 μg/mL gentamycin, and 1.5 μg/mL amphotericin B). All cultures were refreshed every 3–4 days.

After 14 days of osteogenic culture on the implants, monocytes were seeded into non-adherent 24-well plates as described in Section 2.2.3 with coculture medium consisting of αMEM, 10% heat inactivated FBS, 50 μL/mL gentamycin, 0.25 μg/mL amphotericin B, 25 ng/mL M-CSF, and freshly added supplements: 0.1 mM L-ascorbic acid 2-phosphate and 10 mM sodium-β-glycerophosphate. Monocytes were allowed to attach for 24 h at 37°C and 5% CO_2. A pilot experiment was performed to determine the composition of the coculture medium, as described in Appendix A.1.

PET Transwell inserts with 8 μm pore size (Greiner Bio-One, Kremsmünster, Austria) were then carefully placed on top of the monocyte-containing wells. Each well was refreshed with 600 μL fresh coculture medium, and 400 μL of the same medium was pipetted into each Transwell. The hMSC-seeded implants were transferred into the Transwell inserts using sterilised forceps. Cocultures were maintained for 11–14 days, with medium refreshed every 3–4 days.

This indirect coculture system enabled the assessment of osteoclastogenesis in response to hMSC-conditioned environments generated on PEO and PEO+AgNP implant surfaces, without direct monocyte–implant contact.

2.4 Monocyte and osteoclast viability

Viability of monocytes cultured with or without M-CSF, as well as monocytes differentiated into osteoclasts directly on the implant surfaces, was assessed using a Live/Dead Viability/Cytotoxicity assay (Gibco, ThermoFisher Scientific, Breda, The Netherlands). Monocyte viability was evaluated after 4 days of culture, whereas osteoclast viability was assessed after 10 days.

Prior to staining, the samples were rinsed three times with 0.9%(w/v) NaCl to remove non-adherent cells and residual medium. The implants were then incubated in a staining solution consisting of 0.1% Calcein-AM and 0.15% Ethidium homodimer-1 (EthD-1) prepared in 0.9% NaCl. Samples were incubated in the dark for 40 min at 37°C to prevent photobleaching and ensure accurate fluorescent signal development.

Following incubation, the samples were gently rinsed again with 0.9% NaCl and immediately imaged using a fluorescence microscope (Echo Revolve R4, Echo, San Diego, USA). Viable cells emitted a bright green fluorescent colour, while the dead cells showed a red colour. This allowed qualitative assessment of cell attachment and survival on PEO and PEO+AgNP implant surfaces under different culture conditions.

2.5 DNA quantification

To obtain a quantitative measure of monocyte attachment on the implant surfaces under conditions with and without M-CSF, DNA content was assessed using the CyQUANT Cell Proliferation Assay Kit (Gibco, ThermoFisher Scientific, Breda, The Netherlands).

Following culture, the cells were covered with a papain digestion solution consisting of papain buffer (0.2 M NaH_2PO_4, 0.01 M EDTA·$2H_2O$, ph=6.0), 0.01 M cysteine HCl, and 250 μg/mL papain. Samples were incubated overnight in a 60°C water bath to ensure complete enzymatic digestion of cellular material.

A DNA standard curve was prepared according to the manufacturers instructions. For each sample, 50 μL of digested lysate and standards ranging from 0 to 62.5ng DNA were pipetted into a black, microclear 96 flat bottom well plate in duplicate. Subsequently, 75 μL of RNase/heparin solution (8.3 IU/ml Heparin, 50 microgram/ml RNase) was added to each well to degrade RNA and prevent DNA aggregation. The plate was incubated for 30 min at 37°C.

Following incubation, 30 μL of diluted (1:400) CyQUANT GR dye solution was added to each well, and fluorescence was measured using a SpectraMax iD3 microplate reader (Molecular Devices, San Jose, California, USA) at 480 nm excitation and 520 nm emission. DNA concentrations were calculated from the standard curve, enabling quantitative comparison of monocyte attachment between experimental groups.

2.6 Osteoclast visualisation and quantification

Osteoclast formation in mono- and coculture conditions was assessed using tartrate-resistant acid phosphatase (TRAP) staining. Cells were harvested after 11–14 days of culture, using three biological donors in triplicate. The variation in harvesting time resulted from differences in differentiation speed between donors; two donors reached full differentiation by day 11, and extending culture to day 14 posed a risk of osteoclast degradation. CD14+ monocytes merge and differentiate into osteoclasts. However, these artificial osteoclasts have a limited lifespan.

For staining, samples were first rinsed with PBS and subsequently fixed in 4% formalin for 1 h at room temperature. After fixation, the cells were washed three times in PBS and three additional times in demineralised water for 5 min each. Samples were then incubated for 20 min in freshly prepared acetate–tartaric acid buffer (0.2 M sodiumacetate, 100 mM L(+)tartaric acid, adjusted to pH 5 using 10 M NaOH).

A TRAP staining solution was prepared by mixing 0.5 mg/mL naphthol AS-BI phosphate (Sigma-Aldrich, St. Louis, Missouri, USA) with 1.1 mg/mL Fast Red TR salt (Sigma-Aldrich, St. Louis, Missouri, USA) in the acetate–tartaric acid buffer. Samples were covered with the staining solution and incubated on a orbital shaker at 37°C for 15–30 min. Staining progression was monitored under a light microscope starting at 15 min and subsequently every 5 min. Once osteoclasts dis-

played a distinct bright pink colour, the reaction was stopped by rinsing samples thoroughly in distilled water. Hematoxylin was used as a counterstain to visualise the nuclei. All samples were imaged using brightfield light microscopy.

Quantification of osteoclast area coverage was performed using ImageJ in combination with the Stitching and Labkit plugins. For each sample, four TRAP-stained images were stitched to increase the analysed area (Figure 2.5A). Using Labkit, osteoclasts were segmented from the background to generate a binary mask (Figure 2.5B). Osteoclast coverage was quantified by analysing the binary images generated in Labkit, where osteoclasts appeared as white regions (Figure 2.5C). The percentage of white pixels relative to the total image area was calculated, yielding a quantitative measure of osteoclastogenesis for each condition.

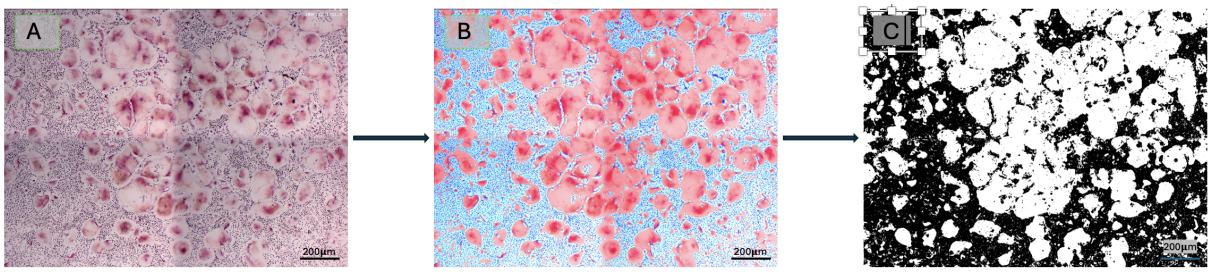

Figure 2.5. The process of quantifying the osteoclast well coverage: (A) Stitched images of the TRAP stained well. (B) Differentiated osteoclasts (red) from the background (blue). (C) Binary image of the osteoclasts (white) used to measure the area covered by osteoclasts.

2.7 Gene expression analysis of osteoclasts

Gene expression analysis was performed on samples from the mono- and coculture conditions harvested on days 10–14 (Figure 2.6). Cells were lysed using 400 µL of RNA-STAT-60 (Tel-Test, Friendswood, Texas, USA). For RNA extraction, 80 µL of chloroform was added to each lysate, followed by centrifugation at 12,000 g for 15 min to accelerate phase separation. The aqueous phase was carefully transferred to a new tube and mixed with an equal volume of 70%(v/v) ethanol.

RNA purification was carried out using Epoch Life Science Mini Spin Columns (#1940-250, Epoch Life Science) (Figure 2.6). Samples were loaded onto the columns and centrifuged at 8,000 g for 30 s. Flow-through was discarded, and the columns were washed sequentially with RW1 buffer (Qiagen, cat. 1053394) and DNase solution (DNase with RDD buffer; Qiagen, cat. 1018013). The RNA bound on the columns was washed with RW1 buffer to remove salts. Resid-

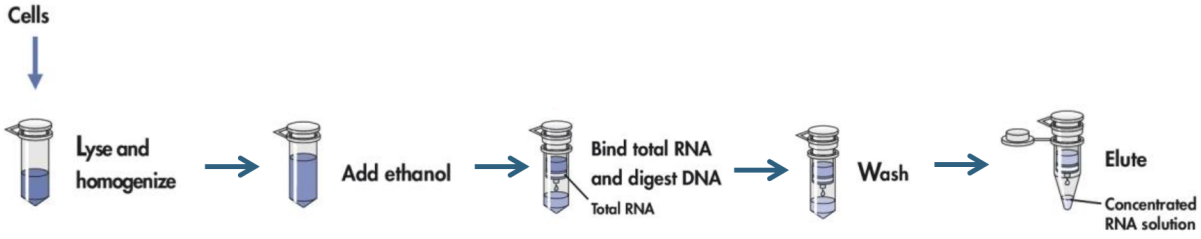

Figure 2.6. Schematic overview of the steps involved in the RNA extraction process.

ual DNA was removed with 30 Kunits units RNase-free DNase I according to the manufacturers instructions. Furthermore the RNA was washed with subsequently RW1, RPE and 80%(v/v) Ethanol to remove salts. RNA was finally eluted in RNase-free distilled water. All centrifuge steps were executed at 8.000g.

Total RNA concentration and purity were determined using a DSS-11 spectrophotometer/fluorometer (DeNovix, Wilmington, USA) at 260/280 nm. For cDNA synthesis, 0.2 µg RNA per sample was used, following the manufacturer's protocol of the RevertAid First Strand cDNA Synthesis Kit (Thermo Fisher Scientific, Waltham, Massachusetts, USA). After synthesis, 100µL ddH_2O was added to each sample.

Quantitative PCR (qPCR) was performed using either TaqMan (Gibco, ThermoFisher Scientific, Breda, The Netherlands) or SYBR Green 2 × mastermix (Gibco, ThermoFisher Scientific, Breda, The Netherlands). Each reaction contained 5 µL mastermix, 0.5 µL primer+probe mix, and 2 µL cDNA in a 96-well PCR plate. Amplification was carried out using a Bio-Rad CFX96 Real-Time PCR Detection System (Bio-Rad, Hercules, California, USA). Target genes included osteoclast markers such as *TRAP*, *CTSK*, *ATP6V0D2*, *MMP9*, *OC-STAMP*, and *DC-STAMP*. Primer sequences are listed in Table 2.1.

Table 2.1. Primer sequences for the genes used in the qPCR analysis.

Type of gene	Target gene	Forward Sequence (5'-3')	Backward Sequence (5'-3')	Probe (FAM, 5'-3')
Housekeeper	B2M	TGCTCGCGCTACT CTCTCTTT	TCTGCTGGATGACG TGAGTAAAC	
	UBC	ATTTGGGTCGCGG TTCTTG	TGCCTTGACATTCT CGATGGT	
	GAPDH	ATGGGGAAGGTG AAGGTCG	TAAAAGCAGCCCT GGTGACC	CGCCCAATA CGACCAAAT
Osteoclast Marker	DC-STAM	AAGCAGCCGCTGG GAGT	TTTTCAGGACTGGA AGCCAGAAATGAA	
	OC-STAMP	GCCTGAAACCACT GCCATTTG	AGGACCTCCACCCG GTCT	
	ATP6V0D2	TTCTTGAGTAGGC CGACA	AGAGTTTGCCGAA GGTTGGA	
	CTSK	GGGAGCTATGGAA GAAGACCC	CCAAGGTGGTTCATA GCCAGT	
	TRAP	GACTGTGCAGTC CTGGGTG	GAGCGGTCAGAGA ATACGTCC	
	MMP9	TGAGAACCAATC TCACCGACAG	TGCCACCCGAGTGT AACCATGTAACCAT	CAGCTGGCAGAGGA ATACCTGTACCGC

To normalise gene expression across samples, the BestKeeper Index (BKI) was calculated as the geometric mean of the housekeeping genes *GAPDH*, *B2M*, and *UBC*. Relative gene expression was determined using the formula:

$$\text{Gene expression} = 2^{-\Delta C_q}$$

where

$$\Delta C_q = C_{q,\text{sample}} - C_{q,\text{BKI}}$$

2.8 Calcium concentration in culture medium

To assess osteogenic activity of hMSCs cultured on PEO and PEO+AgNP implants, calcium concentration in the culture medium was quantified over time. Medium samples were collected from three technical replicates on every 3-4 days and stored at $-20°C$ until analysis.

A standard curve was prepared using $CaCl_2$ dissolved in calcium-free DMEM at final concentrations of 3, 2, 1.5, 0.75, 0.375, 0.188, 0.093, and 0 mM. For each sample, 10 µL of medium was mixed with 100 µL of a colorimetric reagent prepared as a 1:1 (volume to volume) mixture of 1 M ethanolamine (pH 10.5) and 0.35 mM o-cresolphthalein complexone and 19.8 mM 8-hydroxyquinoline dissolved in 0.6 M hydrochloric acid (all reagents from Sigma-Aldrich, St. Louis, Missouri, USA).

Calcium concentration was determined by measuring absorbance at 570 nm using a VersaMax Microplate Reader (Molecular Devices, San Jose, California, USA). Sample concentrations were calculated by fitting absorbance values to the standard curve and expressed as corrected calcium levels relative to baseline medium controls.

2.9 Statistical analysis

All quantitative data were analysed using a linear mixed-effects modelling approach. A Linear Mixed Model (LMM) was chosen to account for the hierarchical structure of the data, in which multiple measurements were obtained from biological donors across different experimental conditions. In all models, experimental condition was treated as a fixed effect, while donor was included as a random effect to account for inter-donor variability and non-independence of observations.

Prior to statistical analysis, data distributions were assessed for normality. Normality was evaluated using visual inspection of histograms and Q–Q plots, as well as formal normality testing. In all cases, the data met the assumptions of normality, and no data transformation was required.

When a significant main effect was detected, pairwise comparisons between conditions were performed with correction for multiple testing. Statistical significance was defined as $p < 0.05$. All statistical analyses were performed using SPSS.

Results 3

3.1 Surface biofunctionalisation of Ti6Al4V implants

The PEO process successfully modified the Ti6Al4V implant surfaces, as indicated by the increase in the voltage during the process (Figure 3.1). SEM imaging revealed that the PEO treated surfaces consisted of micro- and nanopores with diameters up to several micrometres (Figure 3.2A-F). Incorporation of silver nanoparticles into the electrolyte did not noticeably alter the voltage–time transients (Figure 3.1) nor the overall surface morphology when compared with PEO-only implants.

Elemental analysis using EDS confirmed the presence of Ti and Al from the alloy substrate, as well as Ca, P, O, and Ag on the PEO treated surfaces (Figure 3.2G-I). The detection of calcium and phosphorus indicates that calcium and phosphate components from the electrolyte had become embedded within the growing oxide layer, while clear Ag peaks in the spectra verified the presence of silver in the PEO+AgNP layers. These observations confirmed that AgNPs were successfully embedded within the porous PEO layers without altering the characteristic surface topography.

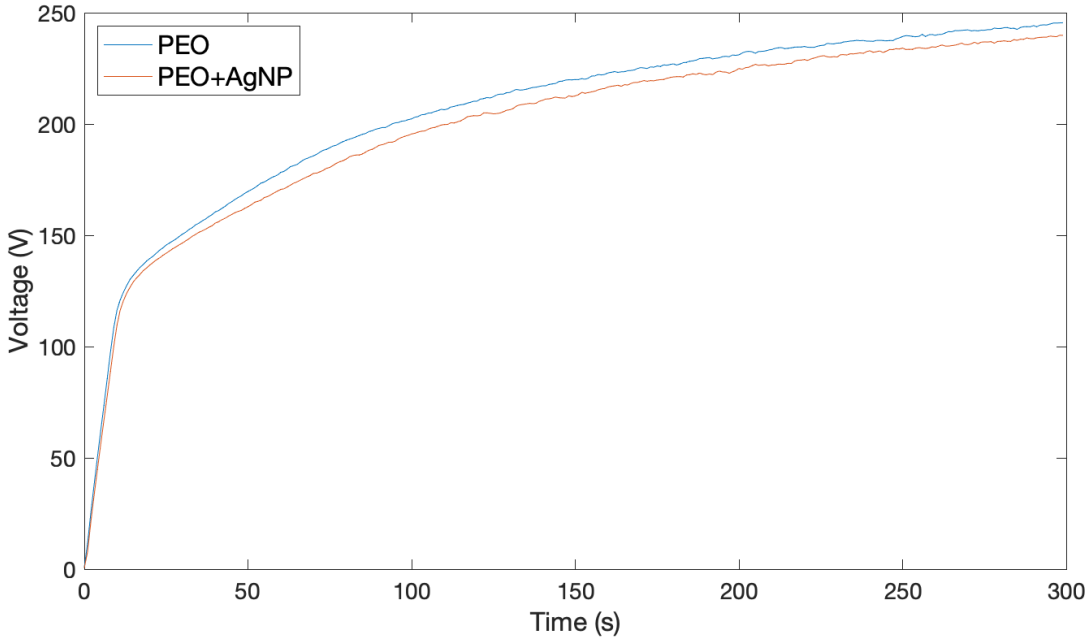

Figure 3.1. Representative voltage transients for PEO and PEO+AgNP implants recorded during the PEO process.

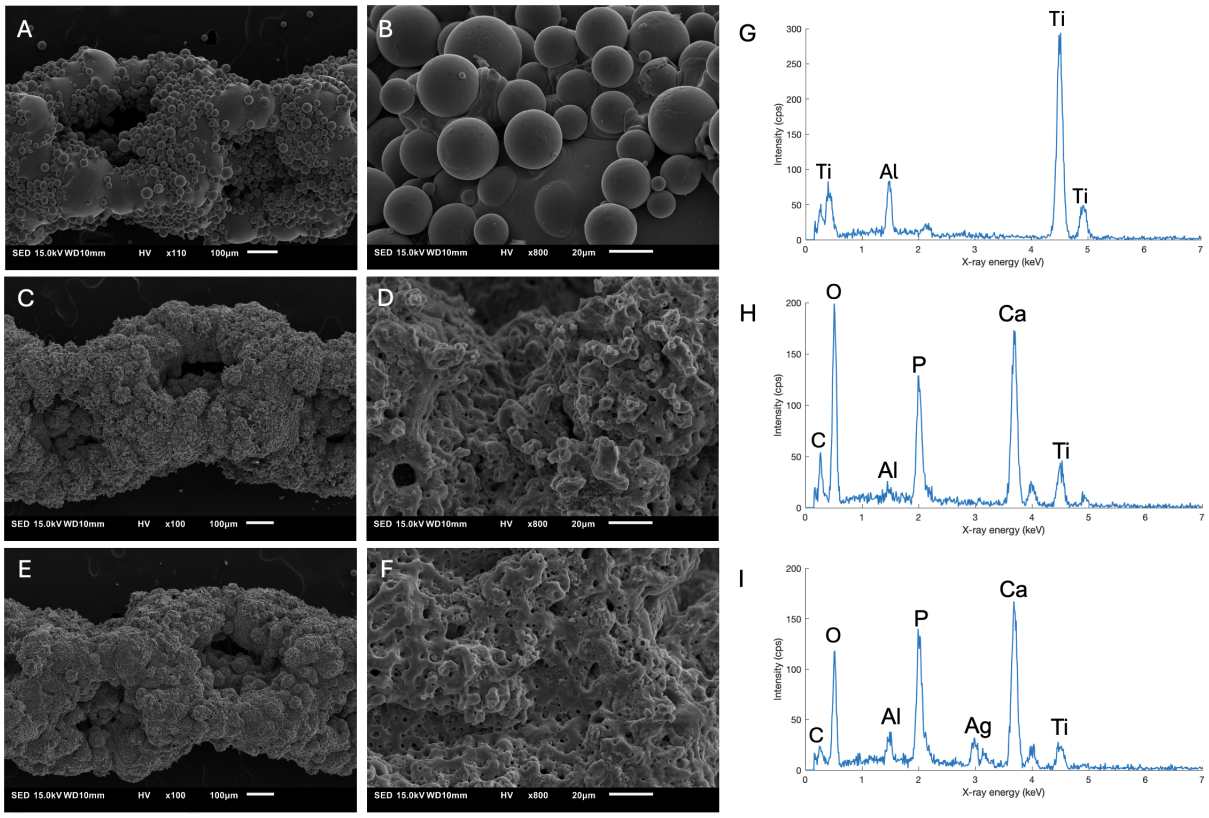

Figure 3.2. Surface characterisation. (A,B) SEM images of the Ti6Al4V non-treated implants. (C,D) SEM images of the PEO implants. (E,F) SEM images of the PEO+AgNP implants. (G-I) Corresponding EDS analysis.

3.2 Effects of M-CSF in culture medium on monocyte viability

The influence of M-CSF supplementation on monocyte attachment and survival was assessed after 4 days of culture on PEO-treated implants. Live/Dead fluorescence imaging (Figure 3.3A-B) showed a higher number of viable cells on samples cultured with M-CSF.

This observation was confirmed by DNA quantification (Figure 3.3C), which revealed a significant decrease in DNA content in the absence of M-CSF ($p < 0.001$). Together, these findings

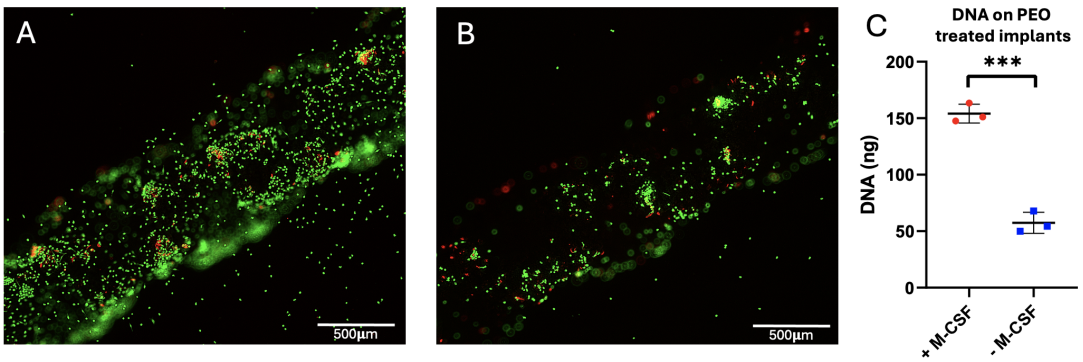

Figure 3.3. (A,B) Representative Live/Dead images of PEO implants seeded with CD14+ monocytes and cultured for 4 days with and without M-CSF in the culture medium. (C) DNA quantification of CD14+ monocytes seeded and cultured on PEO implants with and without M-CSF. p<0.001 (***)

demonstrate that M-CSF is essential for maintaining monocyte viability under the applied culture conditions.

3.3 Effects of AgNPs incorporated in PEO treated implants on osteoclast viability

The effect of AgNP-containing implant surfaces on monocyte differentiation into osteoclasts was evaluated by culturing monocytes from one donor (three technical replicates per condition) directly on non-treated, PEO, and PEO+AgNP implants for 10 days. Firstly, Live/Dead fluorescence imaging (Figure 3.4A–C) showed that cells were able to attach and survive on all implant types; however, a visibly reduced number of adherent cells was observed on PEO+AgNP implants compared with both non-treated and PEO surfaces.

Osteoclast differentiation was then assessed by analysing the expression of established osteoclast-related genes representing complementary stages of osteoclastogenesis and functional maturation (*TRAP*, *OC-STAMP*, *DC-STAMP*, *CTSK*, and *ATP6V0D2*) (Figure 3.4D). TRAP was included as a canonical marker of osteoclast lineage commitment, while CTSK was analysed as a key protease involved in degradation of the organic bone matrix [15]. ATP6V0D2 was selected due to its essential role in extracellular acidification during bone resorption [26].

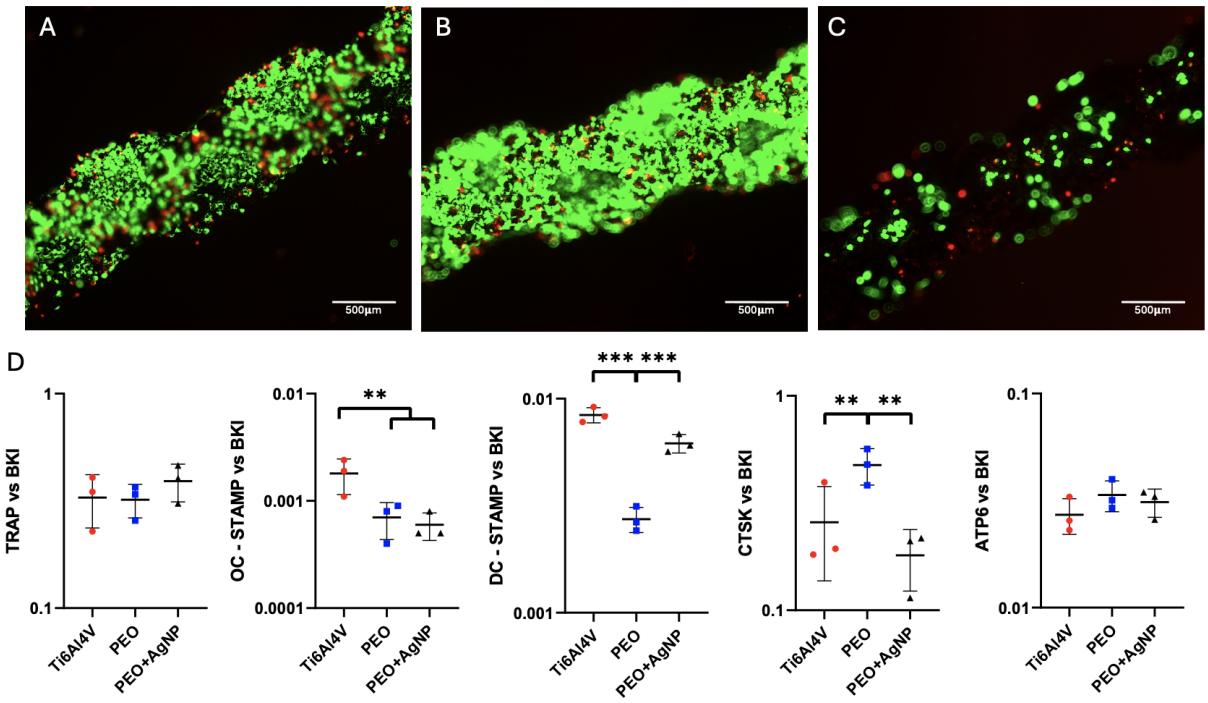

Figure 3.4. CD14+ monocyte differentiation into osteoclasts on different implants surfaces. (A) Live/Dead image of cells cultured on Ti6Al4V non-treated implants. (B) Live/Dead image of cells cultured on PEO implants. (C) Live/Dead image of cells cultured on PEO+AgNP implants. (D) Gene expression levels of osteoclast related genes for cells cultured on different implant surfaces. $p<0.001$ (***), $p<0.03$ (**)

In addition, OC-STAMP and DC-STAMP were analysed as critical regulators of osteoclast pre-

cursor fusion and multinucleation [27, 28]. No clear differences between surface types were detected. *OC-STAMP* expression was higher on non-treated Ti6Al4V compared with the PEO and PEO+AgNP groups ($p < 0.03$), while *CTSK* expression was higher on PEO implants ($p < 0.03$). *DC-STAMP* expression was significantly reduced on PEO implants compared with the other groups ($p < 0.001$). No significant differences were observed for *TRAP* or *ATP6V0D2*.

These findings indicate that while AgNP-containing surfaces reduced overall cell viability, neither PEO treatment nor AgNP incorporation produced consistent differences in osteoclast-related gene expression. Importantly, all groups showed expression of osteoclastic markers, confirming that the cells which survived on each implant type were still capable of differentiating toward osteoclasts.

3.4 Effects of silver ion release from PEO-treated implants on osteoclastogenesis

To assess how silver ion release from AgNP-containing implants influences osteoclastogenesis without direct cell–implant contact, monocytes from three donors were cultured in monolayer while implants were placed in Transwell inserts above the cells. For each donor, cells were cultured in triplicate. A monocyte-only culture without implants or Transwells was cultured on tissue culture plastic and served as a positive control. TRAP staining confirmed that osteoclast formation occurred in all groups (Figure 3.5A–E).

In contrast to the direct-contact experiment (Section 3.3), monocytes exposed to ions released from PEO+AgNP implants showed an osteoclast area coverage comparable to the control group and higher than that of the PEO groups (Figure 3.5F). Quantification confirmed that the PEO and PEO presoaked groups exhibited significantly reduced TRAP-positive area compared with the control, PEO+AgNP, and PEO+AgNP presoaked groups ($p < 0.001$ and $p < 0.01$, respectively), while pre-soaking had little effect, as presoaked and non-presoaked samples produced similar outcomes. These overall trends were consistent across the three donors, despite the expected donor variability.

Gene expression analysis supported the morphological observations. All experimental groups expressed osteoclast-related genes, consistent with the identification of multinucleated TRAP-positive cells as osteoclasts (Figure 3.6). The PEO group exhibited lower expression levels of OC-STAMP and TRAP compared with the PEO+AgNP presoaked and control groups, respectively ($p < 0.05$). These differences indicate altered expression of selected osteoclast-associated markers in the presence of PEO-treated implants.

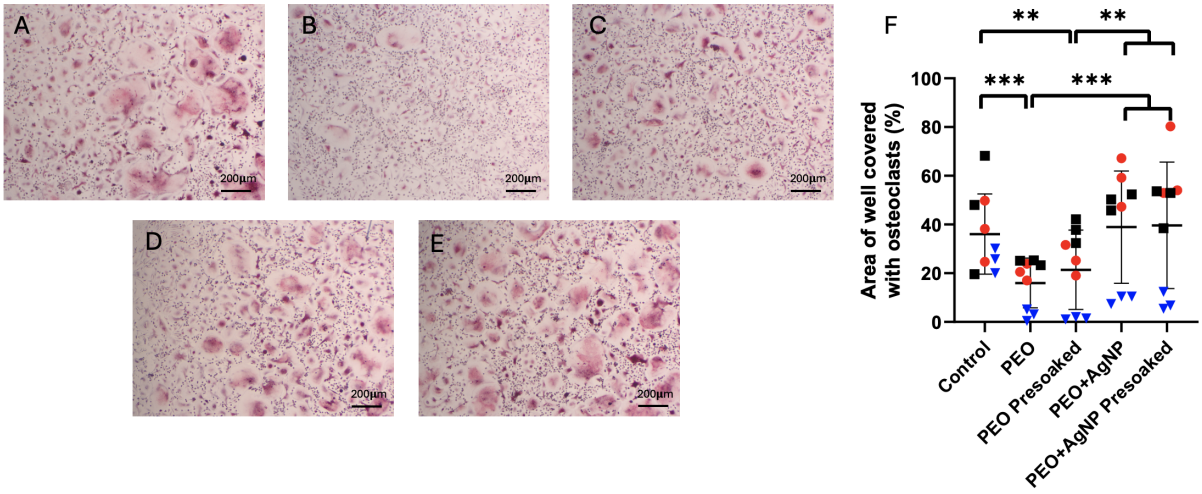

Figure 3.5. (A-E) Representative images of TRAP-stained samples for monocytes cultured in the presense of different implants: (A) control, (B) PEO, (C) PEO presoaked, (D) PEO+AgNP, (E) PEO+AgNP presoaked. (F) Quantified area covered by osteoclasts in different experimental conditions. $p<0.001$ (***), $p<0.01$(**)

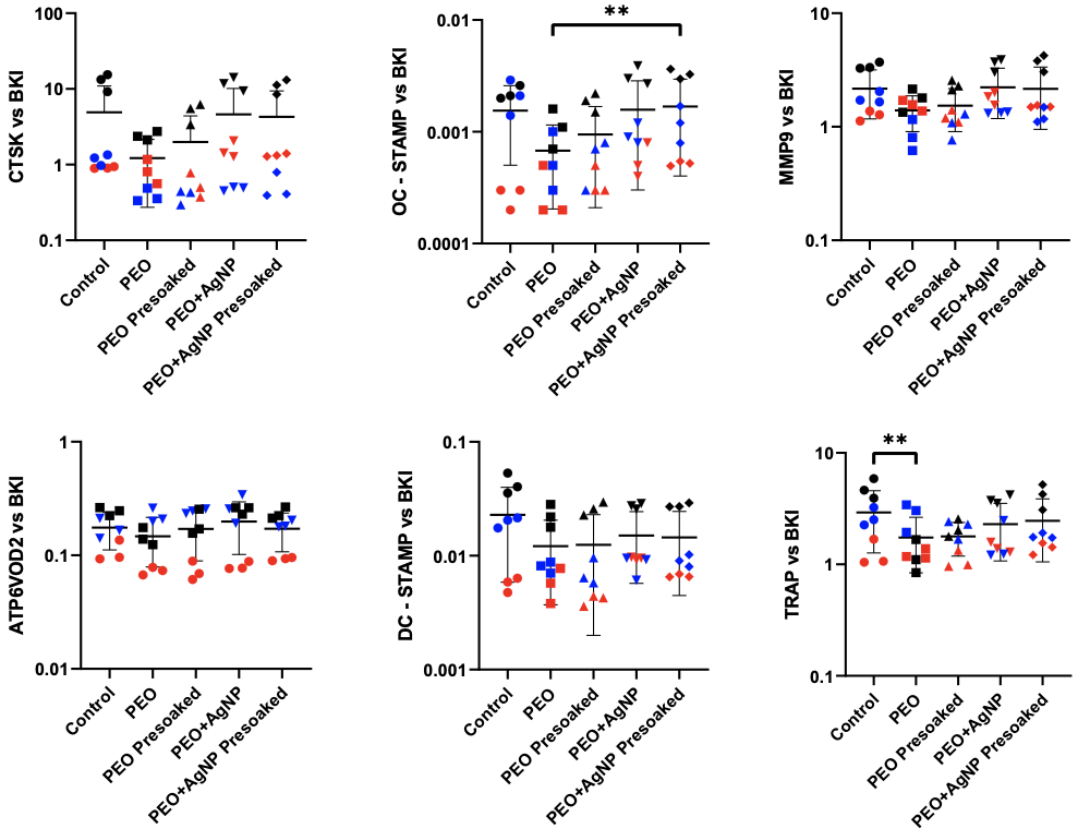

Figure 3.6. Gene expression levels of osteoclast related genes in CD14+ monocytes cultured in the presense of Ti6Al4V non-treated, PEO, and PEO+AgNP implants. $p<0.05$ (**)

3.5 Effects of AgNPs incorporated in PEO treated implants on osteoclast viability when cocultured indirectly with hMSCs

To investigate how silver ion release from AgNP-containing implants influences osteoclastogenesis in the presence of osteogenically differentiated hMSCs, a Transwell-based coculture system was employed in which monocytes were not in direct contact with the implant surface or the hMSCs. hMSCs from three donors were cultured directly on PEO and PEO+AgNP implants for 14 days under osteogenic conditions. Following osteogenic differentiation, the implant-seeded hMSCs were transferred into Transwell inserts and placed above monocytes from three donors, thereby preventing direct monocyte–implant contact while allowing exchange of soluble factors. All donor–implant combinations were cultured in triplicate, and cocultures were maintained for an additional 11–14 days in coculture medium to allow osteoclast formation.

TRAP staining confirmed that osteoclast formation occurred in both PEO and PEO+AgNP groups (Figure 3.7A–B). Quantification of TRAP-positive area showed that wells containing PEO+AgNP implants exhibited more osteoclast coverage compared with the PEO group ($p < 0.005$) (Figure 3.7C). These results indicate that the presence of AgNPs—despite their known cytotoxic potential in direct-contact settings did not impair osteoclastogenesis when only PEO+AgNP and hMSC-derived soluble factors were present.

Gene expression analysis of osteoclasts following coculture showed that both the PEO and PEO+AgNP groups expressed all osteoclast-related genes analysed (Figure 3.7D). Only minimal differences were detected between the two conditions, and no statistically significant changes were observed apart from a small reduction in *OC-STAMP* expression in the PEO+AgNP group ($p < 0.05$). Overall, the gene expression profiles support the TRAP staining results, demonstrating that osteoclasts formed in both conditions and that AgNP-containing implants did not negatively affect osteoclast differentiation in this coculture setup.

To evaluate osteogenic activity of the hMSCs cultured on the implants prior to coculture, calcium concentration in the medium was measured (Figure 3.8). A reduction in Ca^{2+} concentration at days 10 and 14 was observed compared with the media controls for both implant types, consistent with calcium incorporation during matrix mineralisation and indicating successful osteogenic differentiation on both surfaces.

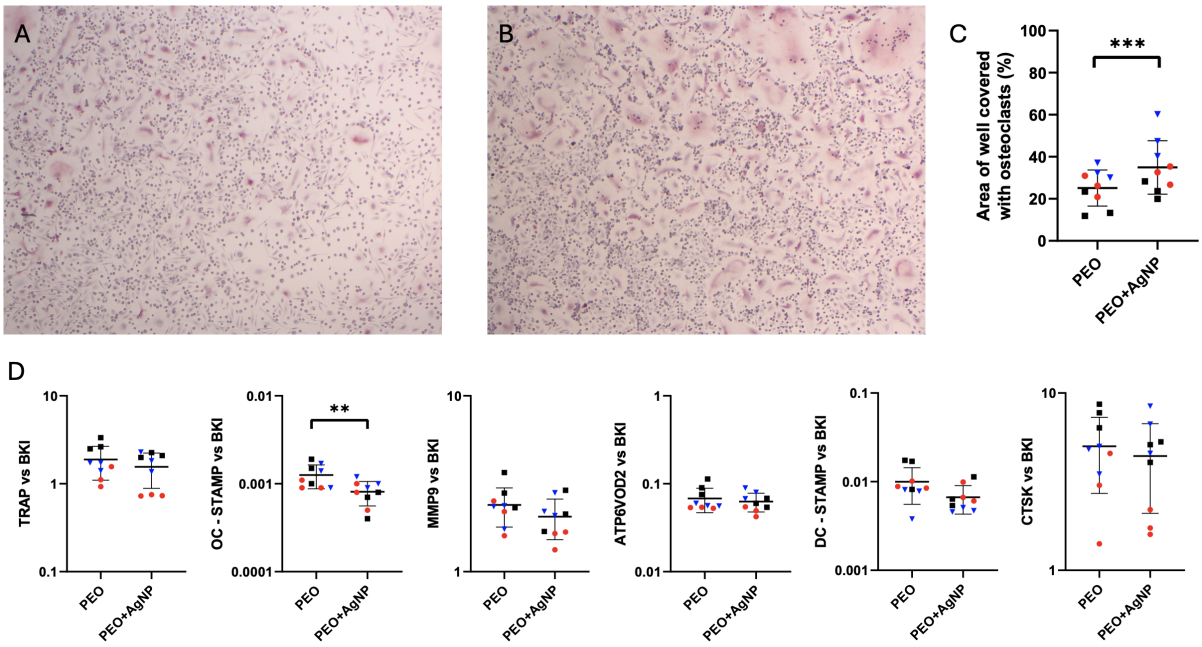

Figure 3.7. Representative images of TRAP-stained samples for monocytes cocultured in the presence of (A) PEO and (B) PEO+AgNP implants. (C) Quantified area covered by osteoclasts in different experimental conditions. (D) Gene expression levels of osteoclast related genes in CD14+ monocytes cultured in the presence of PEO and PEO+AgNP implants precultured with hMSCs for 14 days. $p<0.05$ (**), $p<0.005$ (***)

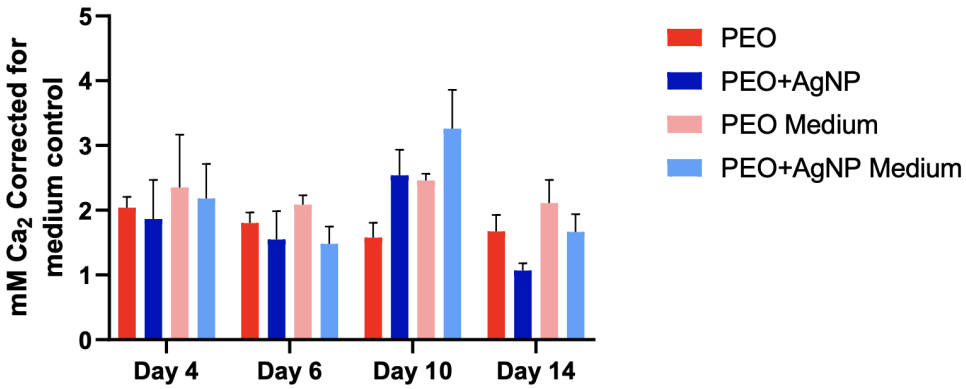

Figure 3.8. Concentration of Ca^{2+} in culture medium for hMSCs cultured on PEO and PEO+AgNP implants.

Discussion 4

The incorporation of antimicrobial agents into orthopaedic implant surfaces is increasingly explored as a strategy to mitigate implant-associated infections while limiting adverse effects on peri-implant tissue responses. Among these agents, AgNPs have attracted sustained interest due to their broad-spectrum antibacterial activity, multi-target mechanism of action, and relatively low tendency to induce bacterial resistance. The antimicrobial function of silver at implant surfaces is closely associated with ion release, which contributes to antibacterial activity while also interacting with surrounding bone regeneration processes. While osteoblast responses to silver-modified surfaces have been studied before, the effects on osteoclasts remain comparatively underexplored.

The present work investigated how AgNPs incorporated into PEO-treated Ti6Al4V surfaces influence osteoclast viability and differentiation under direct and indirect (co)culture conditions. By combining surface characterisation, controlled in vitro culture models, and human primary cells, this thesis aimed to clarify whether antimicrobial surface biofunctionalisation can be achieved without compromising osteoclast-related processes critical for human bone regeneration and remodelling. In direct contact cultures, PEO+AgNP surfaces were associated with a reduced number of adherent viable osteoclast precursors compared with PEO-only implants, although osteoclast-related gene expression remained detectable in the surviving cells. In contrast, under indirect exposure conditions, AgNP-containing implants did not impair osteoclast formation and, relative to PEO-only surfaces, showed comparable or increased osteoclastogenesis. These findings indicate that the effects of AgNP incorporation are strongly dependent on the type of exposure.

4.1 Surface biofunctionalisation of Ti6Al4V implants

PEO treatment enabled the successful incorporation of AgNPs into the oxide layer of Ti6Al4V substrates, producing a porous, microstructured surface capable of hosting antimicrobial agents. Such surface architectures are well-established for improving implant bioactivity while enabling controlled release of incorporated species [10, 23]. In the present study, AgNP incorporation did not alter the characteristic PEO morphology, suggesting that silver addition was compatible with maintaining surface features relevant for cell–biomaterial interactions.

From a biological perspective, this is important, as surface topography and chemistry are known to influence protein adsorption, immune cell attachment, and subsequent osteoclast precursor behaviour [29, 30]. Because the PEO surface morphology was comparable across groups, major

differences in topographical effects on cell behaviour are unlikely, despite early protein adsorption and immune signalling not being assessed.

4.2 Effects of M-CSF in culture medium on monocyte viability

M-CSF is a critical survival factor for monocytes and osteoclast precursors, supporting their maintenance and differentiation capacity [31]. The observed dependence of monocyte viability on M-CSF supplementation in this study aligns with established osteoclast differentiation protocols and confirms that the experimental system provides the minimal biological support required for precursor maintenance.

Confirming the role of M-CSF in supporting monocyte survival validates the biological integrity of the experimental system. However, cell viability remains influenced by multiple factors, including material properties, and these contributions are considered in the interpretation of subsequent experiments.

4.3 Effects of AgNPs incorporated in PEO-treated implants on osteoclast viability

In the direct-contact model, monocytes were able to attach and undergo osteoclast differentiation on all implant types. However, Live/Dead imaging qualitatively indicated a markedly lower number of viable, adherent cells on the PEO+AgNP surfaces compared with both non-treated and PEO-only implants. This observation suggests that the presence of AgNPs in the PEO coating negatively affected cell attachment and/or survival under direct exposure conditions.

These findings indicate that while AgNP-containing surfaces reduced overall cell viability, neither PEO treatment nor AgNP incorporation produced consistent differences in osteoclast-related gene expression. Importantly, all groups showed expression of osteoclastic markers, confirming that the cells which survived on each implant type were capable of differentiating toward osteoclasts. However, the markedly reduced number of adherent cells on the AgNP-containing surfaces should be considered when interpreting these results, as differences in gene expression may be obscured when fewer cells contribute to the overall signal.

An important consideration is that the direct-contact experiment was performed without presoaking the implants. Because the implants exhibit an initial burst release of ions, pre-soaking the PEO+AgNP implants prior to seeding may have reduced early silver ion peaks and potentially improved initial monocyte attachment and survival. Although this was not evaluated in the present direct-contact model, comparing presoaked and non–presoaked implants in a direct contact model would help to distinguish effects driven by early release kinetics from those caused

by surface-associated AgNPs or other material properties.

Overall, these results support a model in which AgNP-containing PEO surfaces primarily influence cell survival/attachment in direct contact, while osteoclast differentiation of the surviving cells appears broadly maintained within the limits of the markers assessed.

4.4 Effects of silver ion release from PEO-treated implants on osteoclastogenesis

The indirect Transwell-based monoculture model was specifically chosen to decouple the effects of implant derived ions from direct cell–biomaterial interactions, while maintaining relevance to in vivo conditions. By culturing monocytes in monolayer and positioning the implants in Transwell inserts above the cells, osteoclastogenesis could be assessed in response to ions released from the implant surfaces, without confounding influences of surface topography, local AgNP contact, or differences in initial cell attachment.

This approach reflects a clinically relevant separation during the bone regeneration process. While hMSCs are expected to populate the implant surface and contribute to new bone formation, osteoclasts act on the adjacent residual bone surfaces by resorbing necrotic or damaged bone generated during the operation and preparing the interface for subsequent osteoblast mediated matrix deposition and remodelling. In this context, ions released from the implant can diffuse into the local microenvironment and influence osteoclastogenesis without direct osteoclast–implant contact. The Transwell-based setup was therefore chosen to evaluate the effects of implant-derived ions on monocyte-to-osteoclast differentiation in a contact-free manner, complementing the direct-contact model that captures surface-associated effects.

The inclusion of presoaked implant conditions was motivated by the well-documented early burst release of ions from PEO treated surfaces [19], with the aim of reducing initial ion spikes and better approximating in vivo exposure conditions. In vivo, implant-derived ions are continuously diluted and transported away from the implant surface by interstitial fluid flow and blood perfusion, whereas in vitro such ions remain confined within a static culture volume, potentially leading to locally elevated concentrations. From this perspective, pre-soaking may provide a more physiologically representative exposure scenario by partially accounting for ion dilution that would occur in the dynamic in vivo environment. The largely comparable outcomes between pre-soaked and non-pre-soaked conditions suggest that early burst release did not dominate osteoclastogenic responses in the indirect setting. In contrast, under direct-contact conditions, initial ion peaks may have had a greater impact due to local concentration effects at the cell–implant interface, potentially contributing to the reduced cell survival observed.

In contrast to the reduced osteoclast formation observed in the presence of PEO-treated implants alone, indirect exposure to silver-containing surfaces resulted in osteoclastogenesis comparable to control conditions. Quantification of TRAP-positive area indicated that the presence of silver

ions did not suppress osteoclast formation under indirect exposure conditions and, relative to PEO, was associated with increased osteoclast coverage. Gene expression analysis did not reveal major differences in osteoclast-associated markers between conditions, suggesting that the observed effects are not driven by pronounced changes in canonical differentiation pathways.

These findings contrast with studies reporting inhibitory effects of silver ions on osteoclast differentiation, which are frequently associated with cytotoxicity or reduced TRAP-positive osteoclast formation even at low silver ion concentrations [32–34]. Importantly, exposure to silver ions is commonly linked to reduced osteoclast viability, whereas modulation of osteoclastogenesis in the absence of extensive cell death has mainly been reported at low, sub-cytotoxic concentrations. Within this context, the present results suggest that silver ion release from AgNP-incorporated PEO surfaces does not impair osteoclastogenesis under indirect exposure conditions and may mitigate inhibitory effects associated with the PEO surface itself.

These findings should be interpreted within the context of the experimental design. Where no statistically significant differences were detected, the groups can be considered comparable under the tested conditions. Taken together, the data indicate that PEO treatment alone was associated with reduced osteoclast formation in the indirect model, whereas incorporation of AgNPs resulted in osteoclastogenesis comparable to control conditions. These findings suggest that silver incorporation did not impair osteoclast differentiation and may counteract inhibitory effects observed with PEO-only surfaces, although further work is required to clarify the underlying mechanisms.

4.5 Effects of AgNP-incorporated PEO-treated implants under indirect coculture conditions

Including an indirect coculture with hMSCs increased the physiological relevance of the in vitro model by introducing a more complex environment representative of the bone–implant interface. Under indirect exposure conditions, a comparable response was observed in both mono- and cocultures, indicating that the presence of hMSCs did not substantially modify the osteoclast response observed in this experimental setup. The similar responses observed in mono- and coculture conditions therefore suggest that hMSCs did not play a dominant regulatory role in this model.

This similarity suggests that the indirect effects associated with silver ion release remain detectable in a more complex cellular environment. Notably, the reduced osteoclast formation in the PEO-only group was observed in the indirect Transwell setting, suggesting that soluble PEO-derived ions (rather than the PEO surface) may suppress overall osteoclast formation. The relative increase in osteoclast coverage in the PEO+AgNP condition when compared to PEO suggests that silver release may mitigate this indirect PEO-associated effect, rather than directly enhancing osteoclast differentiation. Such observations are consistent with literature indicating that osteoclast behaviour can be directly influenced by biomaterial-derived cues, while still being

influenced by the surrounding cellular environment [30, 35].

Accordingly, the indirect model indicates that silver ion release can influence osteoclast behaviour beyond the immediate implant surface, while other cell-derived signals may also contribute. Differences between direct and indirect outcomes likely reflect that direct culture captures surface-driven attachment and local microenvironment effects, whereas indirect culture isolates the influence of released species on total osteoclast yield. More generally, osteoclast responses to biomaterials reflect the combined influence of multiple cues, which cannot be fully separated within the present study [30].

The calcium concentrations measured in the culture medium exceeded baseline medium values, which may reflect multiple contributing factors. In addition to possible calcium ion release from the PEO treated surfaces [23], evaporation of culture medium during culture may also have contributed to an apparent increase in measured calcium concentration.

4.6 Implications for implant surface design

Taken together, the findings suggest that AgNP incorporation into PEO-treated Ti6Al4V surfaces can provide antimicrobial functionality while maintaining osteoclast viability and only moderately influencing differentiation-related processes. From an implant design perspective, this supports the concept that controlled silver incorporation—particularly when immobilised within surface layers—may offer a viable balance between antibacterial efficacy and bone remodelling compatibility.

It should, however, be acknowledged that direct-contact experiments demonstrated reduced viability of monocytes on PEO+AgNP surfaces, indicating that some precursors that initially encounter the implant may not survive. Importantly, cell attachment was still observed, although in lower numbers. In vivo, the early implant environment is highly dynamic, with continuous recruitment of circulating monocytes, rapid protein adsorption, and fluid-mediated dilution of released ions. Therefore, the extent of early cytotoxic effects may be less pronounced than observed under static in vitro conditions, and a partial reduction in initial monocyte attachment is likely to be compensated by the ongoing recruitment of circulating precursors during the early inflammatory phase.

Crucially, the results reinforce the importance of release kinetics rather than total silver content. Surfaces that promote sustained, low-level ion release are more likely to fall within a biologically tolerable window, whereas uncontrolled or high-dose release may disrupt osteoclastogenesis. This aligns with broader literature emphasizing biomaterial architecture and release behaviour as primary determinants of silver biocompatibility [17, 23].

4.7 Limitations

Several limitations should be acknowledged. First, the study was conducted entirely in vitro, and cellular responses may differ under the complex mechanical, inflammatory, and immune conditions present in vivo. Second, while silver release profiles from PEO and PEO+AgNP treated surfaces have been reported previously, silver ion and other soluble factor concentrations were not directly quantified over time in the present study, limiting precise correlation between release behaviour and biological effects. Third, osteoclast-related outcomes were assessed primarily through viability assays and differentiation markers (TRAP staining and gene expression), without direct measurement of resorptive activity.

Additionally, some observed trends did not reach statistical significance, and these findings should therefore be interpreted cautiously. The indirect coculture model, while informative, does not fully capture the dynamic, multi-cellular environment of the bone–implant interface.

4.8 Recommendations for future work

The present study contributes to the understanding of how AgNP-incorporated PEO-treated Ti6Al4V implants influence osteoclast-related cellular responses under controlled in vitro conditions. Building on previous work within this research line and the findings reported here, several directions for future research can be identified.

- **Functional assessment of osteoclast activity beyond differentiation markers.** In this study, osteoclast responses were primarily evaluated using viability, differentiation markers, and TRAP staining. Future work should include direct measurements of osteoclast resorptive activity, such as pit formation assays, to determine whether the observed cellular responses translate into functional changes in bone resorption.
- **Refinement of coculture models to further resolve osteoclast-specific interactions.** While the present study incorporated osteoclast precursors and osteogenically differentiated hMSCs in an indirect coculture system, future research could expand on this approach by integrating more complex and dynamic coculture models. These may include additional immune cell populations, direct cell–cell contact, or temporally controlled differentiation stages to better capture the coordinated regulation of bone formation and resorption at the bone–implant interface.
- **Translation toward in vivo bone remodelling models.** To fully assess the clinical relevance of AgNP-incorporated PEO surfaces, in vivo studies are required. Animal models that allow simultaneous evaluation of infection prevention, osseointegration, and balanced bone remodelling would provide important confirmation of whether the in vitro findings translate to physiological conditions.

Conclusion 5

This thesis investigated how AgNPs incorporated into PEO treated Ti6Al4V implant surfaces influence osteoclast-related cellular responses under direct and indirect in vitro exposure conditions. Given the clinical need for antimicrobial implant surfaces that do not compromise bone remodelling, the study focused on evaluating osteoclast viability and differentiation in response to both implant surface characteristics and released ions.

PEO treatment successfully generated a porous oxide layer enriched with calcium and phosphate components, and AgNP incorporation was confirmed without altering the characteristic surface morphology. These findings demonstrate that PEO provides a suitable platform for incorporating antimicrobial agents while maintaining surface features relevant for cell–material interactions.

In direct contact culture, monocytes were able to attach and differentiate toward osteoclasts on all implant surfaces. However, AgNP containing PEO surfaces were associated with a reduced number of attached viable cells compared with PEO-only and non-treated implants. Despite this reduction, osteoclast related gene expression was detected across all surface types, indicating that the surviving cells retained the capacity for osteoclast differentiation.

By comparison, when monocytes were not in direct contact with the implant surface in Transwell-based indirect culture models, AgNP-containing PEO implants did not impair osteoclast formation. Osteoclast area coverage and gene expression profiles under indirect exposure were comparable to control conditions and interestingly, relative to PEO-only implants, showed trends toward increased osteoclastogenesis. Similar results were observed in the indirect coculture model incorporating osteogenically differentiated hMSCs, indicating that AgNP-containing implants did not negatively affect osteoclast differentiation in a more complex, cell-mediated environment.

Overall, the results demonstrate that the effects of AgNP-incorporated PEO surfaces on osteoclasts are strongly dependent on the mode of exposure. While direct contact with AgNP-containing surfaces may reduce osteoclast precursor viability, indirect exposure to implant-derived ions does not suppress osteoclastogenesis. These findings support the potential of AgNP-incorporated PEO-treated Ti6Al4V implants to combine antimicrobial functionality with acceptable osteoclast-related responses, provided that silver exposure remains within a biologically tolerable range. Further studies are required to assess functional resorptive activity and to validate these findings in vivo.

References

[1] Dutch Arthroplasty Register (LROI). *LROI Report 2024*. 's-Hertogenbosch, the Netherlands: Dutch Arthroplasty Register, 2024. URL: https://www.lroi.nl/media/prqogokg/pdf-lroi-report-2024.pdf.

[2] E. Marin and A. Lanzutti. "History of Metallic Orthopedic Materials." In: *Metals* 15.4 (2025). DOI: 10.3390/met15040378.

[3] S. Duman et al. "Comparison of clinical characteristics and 10-year survival rates of revision hip arthroplasties among revision time groups." In: *Archives of Medical Science* 17.2 (2021), pp. 382–389. DOI: 10.5114/aoms.2019.88563.

[4] M. Rozis, D. S. Evangelopoulos, and S. G. Pneumaticos. "Orthopedic Implant-Related Biofilm Pathophysiology: A Review of the Literature." In: *Cureus* (2021). DOI: 10.7759/cureus.15634.

[5] C. W. Hall and T. Mah. "Molecular mechanisms of biofilm-based antibiotic resistance and tolerance in pathogenic bacteria." In: *FEMS Microbiology Reviews* 41.3 (2017), pp. 276–301. DOI: 10.1093/femsre/fux010.

[6] Z. Khatoon et al. "Bacterial biofilm formation on implantable devices and approaches to its treatment and prevention." In: *Heliyon* 4.12 (2018). DOI: https://doi.org/10.1016/j.heliyon.2018.e01067.

[7] R. Aguilar-Garay et al. "A Comprehensive Review of Silver and Gold Nanoparticles as Effective Antibacterial Agents." In: *Pharmaceuticals* 17.9 (2024). DOI: 10.3390/ph17091134.

[8] Y. Qing et al. "Potential antibacterial mechanism of silver nanoparticles and the optimization of orthopedic implants by advanced modification technologies." In: *International Journal of Nanomedicine* 13 (2018), pp. 3311–3327. DOI: 10.2147/IJN.S165125.

[9] T. Bruna et al. "Silver Nanoparticles and Their Antibacterial Applications." In: *International journal of molecular sciences* (2021). DOI: 10.3390/ijms22137202.

[10] S. Sikdar et al. "Plasma Electrolytic Oxidation (PEO) Process—Processing, Properties, and Applications." In: *Nanomaterials* 11.6 (2021). DOI: 10.3390/nano11061375.

[11] B.S. Necula et al. "An electron microscopical study on the growth of TiO2–Ag antibacterial coatings on Ti6Al7Nb biomedical alloy." In: *Acta Biomaterialia* 7.6 (2011), pp. 2751–2757. DOI: https://doi.org/10.1016/j.actbio.2011.02.037.

[12] S. Parithimarkalaignan and T. V. Padmanabhan. "Osseointegration: An Update." In: *The Journal of Indian Prosthodontic Society* 13.1 (2013), pp. 2–6. DOI: 10.1007/s13191-013-0252-z.

[13] R. M. Grzeskowiak et al. "Bone and Cartilage Interfaces With Orthopedic Implants: A Literature Review." In: *Frontiers in Surgery* Volume 7 - 2020 (2020). DOI: 10.3389/fsurg.2020.601244.

[14] F. Xu and S. L. Teitelbaum. "Osteoclasts: New Insights." In: *Bone Research* 1.1 (2013), pp. 11–26. DOI: 10.4248/BR201301003.

[15] Q. Xiang et al. "Beyond resorption: osteoclasts as drivers of bone formation." In: *Cell Regeneration* 13.1 (2024). DOI: 10.1186/s13619-024-00205-x.

[16] A. Insua et al. "Emerging factors affecting peri-implant bone metabolism." In: *Periodontology 2000* 94.1 (2024), pp. 27–78. DOI: https://doi.org/10.1111/prd.12532.

[17] M. Fazel et al. "Osteogenic and antibacterial surfaces on additively manufactured porous Ti-6Al-4V implants: Combining silver nanoparticles with hydrothermally synthesized HA nanocrystals." In: *Materials Science and Engineering: C* 120 (2021). DOI: https://doi.org/10.1016/j.msec.2020.111745.

[18] R. B. Foldbjerg et al. "PVP-coated silver nanoparticles and silver ions induce reactive oxygen species, apoptosis and necrosis in THP-1 monocytes." English. In: *Toxicology Letters* 190.2 (2009), pp. 156–162. DOI: 10.1016/j.toxlet.2009.07.009.

[19] A. Garmendia Urdalleta et al. "The response of human macrophages to 3D printed titanium antibacterial implants does not affect the osteogenic differentiation of hMSCs." In: *Frontiers in Bioengineering and Biotechnology* 11 (2023). DOI: 10.3389/fbioe.2023.1176534.

[20] F Razzi et al. "Immunomodulation of surface biofunctionalized 3D printed porous titanium implants." In: *Biomedical Materials* 15.3 (Apr. 2020). DOI: 10.1088/1748-605X/ab7763.

[21] X. Chen et al. "Osteoblast-osteoclast interactions." In: *Connective Tissue Research* 59.2 (2018), pp. 99–107. DOI: 10.1080/03008207.2017.1290085.

[22] I. A. J. van Hengel et al. "Selective laser melting porous metallic implants with immobilized silver nanoparticles kill and prevent biofilm formation by methicillin-resistant Staphylococcus aureus." In: *Biomaterials* 140 (2017), pp. 1–15. DOI: https://doi.org/10.1016/j.biomaterials.2017.02.030.

[23] Ingmar A.J. van Hengel et al. "The effects of plasma electrolytically oxidized layers containing Sr and Ca on the osteogenic behavior of selective laser melted Ti6Al4V porous implants." In: *Materials Science and Engineering: C* 124 (2021). ISSN: 0928-4931. DOI: https://doi.org/10.1016/j.msec.2021.112074. URL: https://www.sciencedirect.com/science/article/pii/S0928493121002137.

[24] D. E. Newbury and Nicholas W. M. Ritchie. "Is Scanning Electron Microscopy/Energy Dispersive X-ray Spectrometry (SEM/EDS) Quantitative?" In: *Scanning* 35.3 (2013), pp. 141–168. DOI: https://doi.org/10.1002/sca.21041.

[25] C. Knuth et al. "Isolating Pediatric Mesenchymal Stem Cells with Enhanced Expansion and Differentiation Capabilities." In: *Tissue Engineering Part C: Methods* 24 (Apr. 2018). DOI: 10.1089/ten.TEC.2018.0031.

[26] H. Wu, G. Xu, and Y. Li. "Atp6v0d2 is an essential component of the osteoclast-specific proton pump that mediates extracellular acidification in bone resorption." In: *Journal of Bone and Mineral Research* 24.5 (2009), pp. 871–885. DOI: 10.1359/jbmr.081239.

[27] M. Yagi et al. “DC-STAMP is essential for cell–cell fusion in osteoclasts and foreign body giant cells.” In: *The Journal of Experimental Medicine* 202.3 (2005), pp. 345–351. DOI: 10.1084/jem.20050645.

[28] M. Yang et al. “Osteoclast stimulatory transmembrane protein (OC-STAMP), a novel protein induced by RANKL that promotes osteoclast differentiation.” In: *Journal of Cellular Physiology* 215.2 (2008), pp. 497–505. DOI: 10.1002/jcp.21331.

[29] J. Barberi and S. Spriano. “Titanium and Protein Adsorption: An Overview of Mechanisms and Effects of Surface Features.” In: *Materials* 14.7 (2021). DOI: 10.3390/ma14071590.

[30] K. Shariati et al. “Biomaterial Cues for Regulation of Osteoclast Differentiation and Function in Bone Regeneration.” In: *Advanced Therapeutics* 8.1 (2025). DOI: 10.1002/adtp.202400296.

[31] K. Fuller et al. “Macrophage colony-stimulating factor stimulates survival and chemotactic behavior in isolated osteoclasts.” In: *The Journal of Experimental Medicine* 178.5 (1993), pp. 1733–1744. DOI: 10.1084/jem.178.5.1733.

[32] C. E. Albers et al. “In vitro cytotoxicity of silver nanoparticles on osteoblasts and osteoclasts at antibacterial concentrations.” In: *Nanotoxicology* 7.1 (2013), pp. 30–36. DOI: 10.3109/17435390.2011.626538.

[33] Z. Wang et al. “Modulating Osteoclast Activity and Immune Responses with Ultra-Low-Dose Silver Nanoparticle-Loaded TiO_2 Nanotubes for Osteoporotic Bone Regeneration.” In: *Journal of Functional Biomaterials* 16.5 (2025). DOI: 10.3390/jfb16050162.

[34] N. Yang et al. “Silver-quercetin-loaded honeycomb-like Ti-based interface combats infection-triggered excessive inflammation via specific bactericidal and macrophage reprogramming.” In: *Bioactive Materials* 43 (2025), pp. 48–66. DOI: 10.1016/j.bioactmat.2024.09.012.

[35] D. Piñera-Avellaneda et al. “Gallium and silver-doped titanium surfaces provide enhanced osteogenesis, reduce bone resorption and prevent bacterial infection in co-culture.” In: *Acta Biomaterialia* 180 (2024), pp. 154–170. DOI: 10.1016/j.actbio.2024.04.019.

Appendix A

A.1 Investigation of a consensus media for a coculture with hMSCs and osteoclasts

To identify a suitable consensus medium supporting both osteogenic differentiation of hMSCs and osteoclast differentiation of monocytes, a preliminary coculture experiment was conducted prior to the main studies. hMSCs were seeded in 24-well plates and cultured in osteogenic medium for 14 days before the introduction of monocytes. Non-osteogenic conditions were included as controls. The samples were refreshed every 3-4 days, and medium samples were collected for the calcium assay.

After 14 days, human CD14+ monocytes were added directly to the hMSC cultures and maintained in one of two candidate coculture media, both supplemented with M-CSF and RANKL. Medium consisting of αMEM, 10% heat inactivated FBS, 50 μL/mL gentamycin, 0.25 μg/mL amphotericin B, and freshly added supplements: 0.1 mM L-ascorbic acid 2-phosphate and 10 mM sodium-β-glycerophosphate. Medium 2 consisted of consisting of αMEM, 10% heat inactivated FBS, 50 μL/mL gentamycin, 0.25 μg/mL amphotericin B, and freshly added 0.1 mM L-ascorbic acid 2-phosphate. A group with monocytes only and osteoclast medium was cultured as well as a control.

Cocultures were maintained for up to 14 days, with medium refreshment performed every 3–4 days. On day 3 of the coculture RANKL was added to the culture medium.

Osteogenic and osteoclastogenic outcomes were evaluated using complementary readouts. Osteoclast formation was evaluated by TRAP staining (Figure A.1A-C), while calcium deposition and mineralisation were assessed by Von Kossa staining (Figure A.1D-F) and calcium concentration measurements in the culture medium (Figure A.1G). Based on these combined readouts, the consensus coculture medium that best supported concurrent osteogenic activity and osteoclast differentiation was selected for subsequent experiments.

No significant differences in hMSC-related outcomes were observed between the tested coculture media. Based on TRAP staining, medium 1 supported the most robust osteoclast formation and was therefore selected for subsequent experiments.

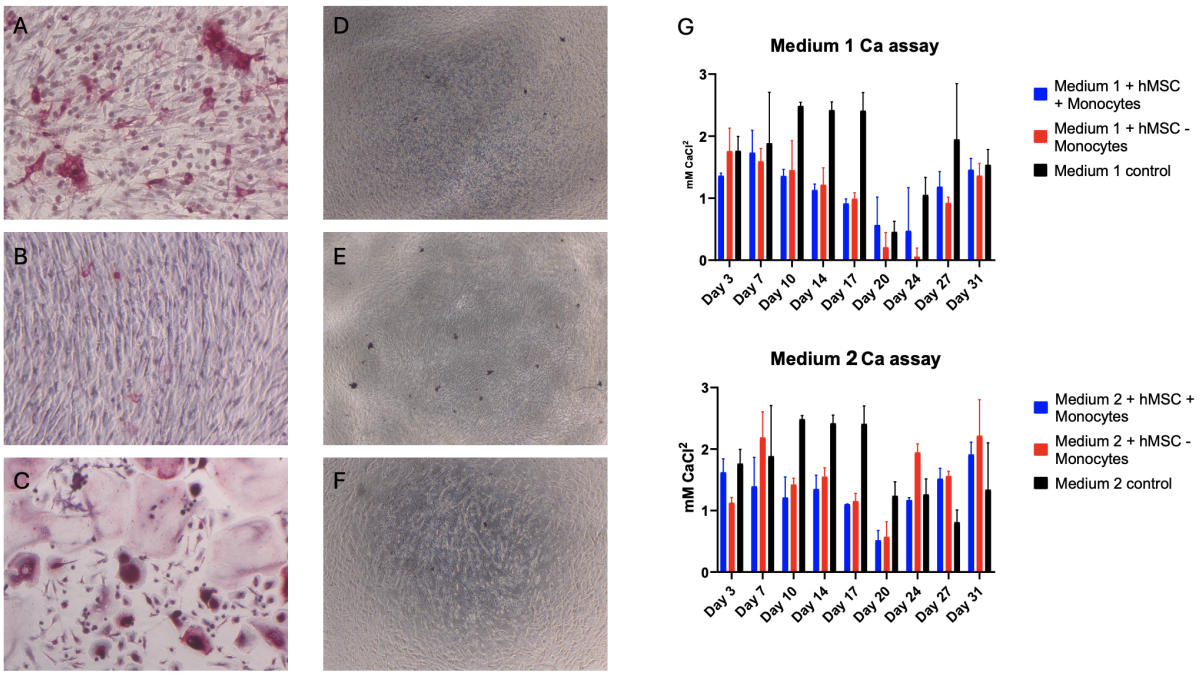

Figure A.1. (A)TRAP staining of coculture in medium 1, (B)TRAP staining of coculture in medium 2, (C)TRAP staining of osteoclast control, (D)Von Kossa staining of coculture in medium 1, (E)Von Kossa staining of coculture in medium 2, (F)Von Kossa Staining of hMSC osteogenic control, (G) Ca assay of hMSCs in medium 1 and 2